Accuracy and Precision of the Z Boson Mass Measurement with the ATLAS Detector

Mariam D'Ciofalo Khodaverdian

Supervisors at the Royal Institute of Technology (KTH):
Christian Ohm, Giulia Ripellino
Teachers of the Natural Science Specialization Course:
Felicia Dinnétz and Per-Olof Freerks
Kungsholmen's Gymnasium
27/05-2019

Abstract

A Toroidal LHC Apparatus (ATLAS) is one of four particle detectors at the Large Hadron Collider (LHC) at CERN. Proton beams accelerated by the LHC enter the detector and collide in ATLAS, which creates new particles that are detected. However, the accuracy and precision of the ATLAS Detector may vary depending on different factors, for example the energies of the particles created. Due to the detector being large, it is also difficult to maintain a homogeneous magnetic field throughout the entire detector. The identification of variations in the accuracy and precision is of great importance to particle physicist working with ATLAS at Cern. As the detector is used to for example search for new particles, the knowledge of the fluctuations in the accuracy and precision must be taken into consideration by operating particle physicists. How does the accuracy and precision in the ATLAS Detector vary as a function of the magnetic field? Using the ATLAS open data samples, a program was written using Python 3 and ROOT. It was investigated how the muon and electron decay channels, pseudorapidity of muons, momentum of muons and momentum of the Z boson affected the accuracy and precision of the ATLAS Detector. In order to identify eventual differences in the accuracy and precision, the mass of the Z boson was calculated for each collision, also referred to as an event, histograms were drawn and the Breit-Wigner and a background function was fitted to the histograms. The parameters obtained were used to identify how the accuracy and precision varied depending on the collision conditions. The center paramameter was compared to the invariant mass of the Z boson and was used to identify fluctuations in the accuracy, and the width parameter was used to analyze the precision of the detector. It was found that the width of the histogram for the muon decay channel was 13.1% narrower than the histogram for the electron decay channel. Additionally, the width of the histogram increased as the pseudorapidity increased. The same trend was observed for the effect of muon momenta on the precision. When the momentum of the Z boson was greater than 20 GeV, the width of the peak increased by 4.4% compared to when it was less than or equal to 20 GeV for the muon decay channels. No difference was observed for the electron decay channels regarding the effect of Z boson momentum on the precision. From this it was concluded that the ATLAS Detector is more accurate and precise for the measurement of muon quantities compared to electron quantities, and that the precision and accuracy decreases as the muon momentum and Z boson momentum increases for the muon decay channel. As the pseudorapidities of the muons increased, the precision decreased, but there was no effect on the accuracy. For the electron decay channel, an increase in Z boson momentum had a negative effect on the precision but no effect on the accuracy. For future investigations, one could narrow the Z boson momentum intervals further to study the topic more in depth.

Key words: *ATLAS Detector, Z boson, precision, accuracy, muon, electron, decay channel, transverse momentum, pseudorapidity.*

Contents

1 Introduction

The Large Hadron Collider (LHC) at Cern (Switzerland) is the biggest particle accelerator in the world with four particle detectors. Proton beams, accelerated to high velocities by the LHC, enter any of the detectors. When the protons collide, new particles are created from the energy in the collision. Some particles created are unstable and decay to other particles. A Toroidal LHC Apparatus (ATLAS) is a particle detector at the LHC that measures quantities, such as momentum and charge, of the particles created during collisions (also referred to as events). However, as the post-collision conditions, such as the particles created and their energies, can vary greatly, the accuracy and precision of the detector fluctuates. In addition to this, the ATLAS Detector measures the quantities using different techniques depending on the particle type, thus certain uncertainties may mostly affect the measurement of certain particles. The Z Boson is an unstable elementary particle that decays before being detected by the ATLAS detector, thus it is the quantities of its decay products that are recorded. The invariant mass of the Z boson can be calculated from its decay products, where the invariant mass is proportional to the inertia of a particle at rest, and remains the same regardless of reference frame (ATLAS experiment, 2019). The invariant mass of the Z boson has been measured many times from experiments, thus a precise value for its invariant mass has been determined by combining the measurements (Ripellino, 2019). By calculating the invariant mass of the Z boson from collisions in the ATLAS Detector and comparing it to the known value, variations in the accuracy and precision of the ATLAS Detector can be identified depending on different post-collision conditions. For this paper, it will be investigated how the magnetic field in the ATLAS Detector affects the accuracy and precision of the detector depending on the decay channel, position of the decay products, muon and Z boson momenta after each collision. This is important in the search of for example new particles and dark matter, as it is something particle physicist must take into consideration and can aid humankind's future understanding of the world and universe. If there are regions in the ATLAS Detector where the measurement is less accurate or precise, or if the accuracy and precision varies depending on how it measures quantities of different particles, the results can help identify these defects and can be used when designing and building new particle detectors. The curiosity for how the smallest components of matter interact with each other and how it is possible to measure them generated the interest to investigate if there are any variations in the accuracy and precision of the ATLAS Detector.

1.1 Research question

How does the accuracy and precision of the ATLAS Detector vary as a function of the magnetic field?

2 Theory

In the standard model, there are two classes of elementary particles, the fermions and the bosons (Hamper, 2014). The fermions are further divided into two groups, the leptons and the quarks. The leptons consist of the electron (e^-), muon (μ^-) and tau (τ^-) particles, each with a negative charge, along with their neutrinos. Both

the leptons and the quarks have antiparticles. Hadrons are composite particles composed of quarks, and consists of the baryons, such as protons, and the mesons (Hamper, 2014). The bosons are mediators of the three fundamental forces. The photon is associated with the electromagnetic force, the gluon mediates the strong nuclear force and the weak nuclear force is mediated by the $W^{\pm}$ bosons and by the Z boson (Hamper, 2014).

The Z boson, Z^0, is a neutral elementary particle. It has a lifetime of 3×10^{-25} s, and decays to a particle and its antiparticle, such as a muon and an anti-muon (see **Fig. 1**), an electron and a positron, a tau and anti-tau and a quark- anti-quark pair (International masterclasses, N/A). Its invariant mass is $Z_m^0 = 91.1872\,\text{GeV}$ (Tanabashi et al., 2019). The tau particle is unstable and there are various decay possibilities. In this paper, only the electron and muon decay channels will be studied, as there are many particles that can decay to quarks.

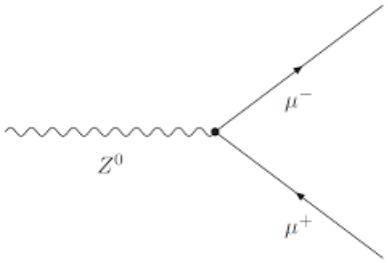

Figure 1: Displays the muon decay channel, where μ^- represents the muon and μ^+ the antimuon (Tripathee, 2017).

The invariant mass of the Z boson can be calculated from the quantities of the two decay products from the equation:

$$m = \sqrt{(2P_{T1}P_{T2}((cosh(\eta_1 - \eta_2) - cos(\phi_1 - \phi_2)))} \quad (1)$$

where P_T is the transverse momentum, η is the pseudorapidity and ϕ, the azimuthal angle, is the angle from the x-axis in the xy-plane measured in radians (see **Fig. 2**). The transverse momentum is the momentum in the xy-plane and the pseudorapidity is a function of θ, $\eta = -ln|tan(\frac{\theta}{2})|$, where θ is defined as the angle from the z-axis in the xz-plane.

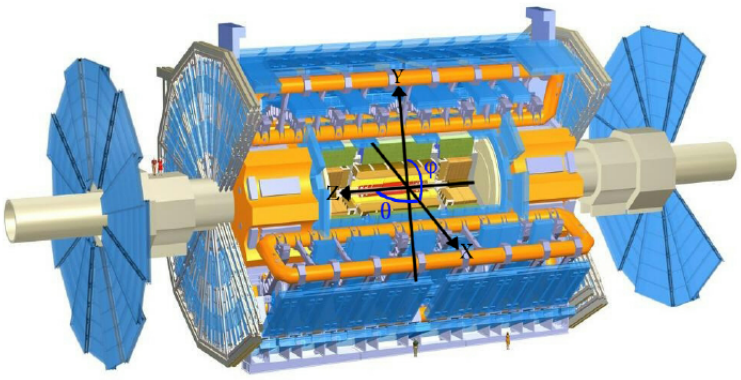

Figure 2: Displays the coordinate system layout in the ATLAS Detector (Hallsjö, 2014).

The LHC at Cern is a particle accelerator that accelerates proton beams to high velocities before the particles enter any of the detectors, such as the ATLAS Detector, where the protons collide and new particles are created from the energy in the collision (Cern, 2019). From one million collisions, only one collision is documented (Cern, 2019). The collisions are selected based on if they are interesting, for example if the particles created have very high transverse momentum (The ATLAS Collaboration et al., 2018). The ATLAS Detector measures the transverse momentum, which is the momentum in the xy-plane, the charge, the pseudorapidity, azimuthal angle and energy of the particles. The detector consists of four different parts that measures the different quantities of the particles created in a collision; the inner detector, two calorimeters and the muon spectrometer (ATLAS experiment, 2019). Using magnetic fields, the inner detector measures the transverse momentum and angle of charged particles by bending their path. The electromagnetic calorimeter consists of materials such as liquid argon, which slows down lighter particles, for example electrons and photons, which are massless (ATLAS experiment, 2019). As the photons and electrons pass the liquid argon they lose energy, which allows the ATLAS Detector to measure their energy. The energies of hadrons are measured in the hadronic calorimeter. Muons, which are heavy, do not lose much of their energy in the calorimeters and are therefore not detected (see **Fig. 3**). The muon spectrometer is thus designed to measure the momentum of the muons using magnetic fields (ATLAS experiment, 2019). In other words, for the electrons and positrons, the quantities are obtained from two measurements, one depending on magnetic fields and one energy measurement, whereas for muons, both of the measurements rely on magnetic fields. As the Z boson has a short lifetime, it is the particles that it has decayed to that are detected by ATLAS, and the mass is calculated from the raw data by equation (1).

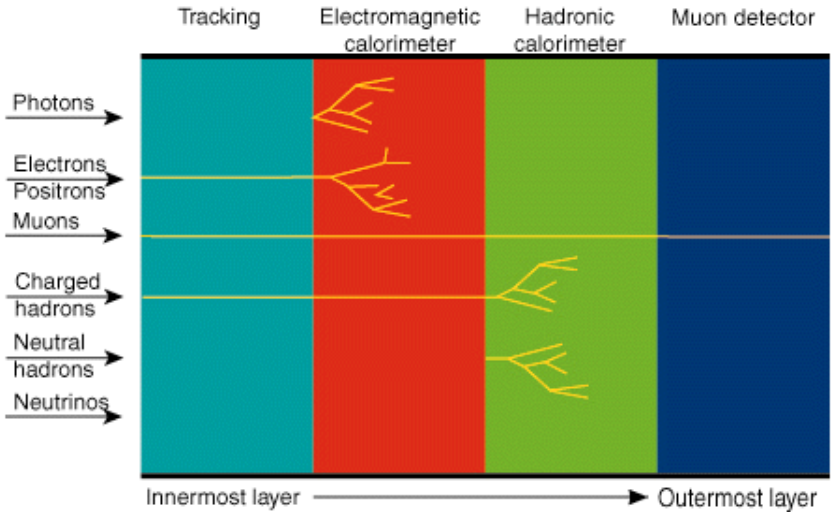

Figure 3: Elementary and composite particles in the four different detector parts (Delmastro, 2012)

The accuracy and precision of the ATLAS Detector varies depending on the collision conditions. It is for example harder to measure the transverse momentum of the particles when it is high, as it becomes more difficult to bend the path using the magnetic field. Additionally, the magnetic fields vary in different regions of the

detector, which can affect the measurement of particle quantities.

The photon decays in the same way as the Z boson, and it is therefore not possible to distinguish events containing either, however, as the photon is massless, it will take on a wide range of values for the invariant mass, whereas the events containing the Z boson will be centred around 91.2 GeV (Ohm & Ripellino, 2019). Furthermore, the J/psi (J/ψ) meson and the upsilon meson can also decay to a muon and one anti-muon or an electron - positron pair (Tanabashi et al., 2019). The J/ψ meson has an invariant mass of 3.096 GeV and the upsilon meson has one of 9.460 GeV (Tanabashi et al., 2019). As both mesons have a lower invariant mass than the Z boson, it will be possible to distinguish them (see section 4.1).

Due to that the invariant mass of the Z boson is precisely known, it can be used to compare the values obtained from this study and from there identify fluctuations in the accuracy and precision. When calculating the invariant mass and drawing it in a histogram, a peak around the invariant mass of the Z boson can be seen. The curve which best follows the shape of the peak is the Breit-Wigner function and the fit of the Breit-Wigner function is an indicator of the accuracy and precision. The center parameter can be used to analyze the accuracy and the width of the peak is of interest regarding the precision as ideally, all entries would fall at 91.2 GeV, thus a wider peak suggests less precision.

3 Methodology

3.1 Event Selection

This study is based on data from the ATLAS Open Data collection, available at `http://opendata.atlas.cern/release/samples/Data` with a total of 14.9×10^6 collisions. In order to enhance the efficiency, a programme was written (see **App. 2**) using Python 3 and ROOT. The following conditions had to be met in order to ensure that events only containing the Z boson were included:

1. There must be two particles detected from each collision.
2. The particles had to be of the same type, that is two muons or two electrons.
3. The particles must have opposite charge (to ensure that the particles are each other's anti particle).

As mentioned in the background, the Z boson, the photon, the J/ψ meson and the upsilon mesons decay in the same way, therefore events in which the photon, J/ψ meson or the upsilon mesons had been created were included and had to be taken into consideration.

To measure how the accuracy and precision varies depending on the magnetic field, the following scenarios were investigated:

1. **Muon and electron decay channels:** Whether a difference exists in the accuracy and precision of the ATLAS detector depending on how it measures different particles, since the detector is more dependent on the magnetic field for measuring the momentum, charge and angles of the muons.

2. **Pseudorapidity:** How the magnetic field varies depending on $|\eta|$. This is only interesting for the muon decay channels, as the muon measurements rely heavily on magnetic fields. Histograms were drawn for the intervals: $|\eta| \leq 0.25$, $0.25 < |\eta| \leq 0.5$, $0.5 < |\eta| \leq 1$, $1 < |\eta| \leq 1.5$ and $|\eta| > 1$ (see **Fig. 4** for some values of η and θ).

3. **Muon momentum:** How the transverse momenta of the muons affects the measurement of muon quantities. This was studied because a particle with higher momentum requires a stronger magnetic field in order to be deflected in the same amount as one with lower momentum. Histograms were drawn for the intervals: $p_T \leq 30\,\text{GeV}$, $30\,\text{GeV} < p_T \leq 40\,\text{GeV}$, $40\,\text{GeV} < p_T \leq 45\,\text{GeV}$, $45\,\text{GeV} < p_T \leq 50\,\text{GeV}$ and $p_T > 50\,\text{GeV}$ (see **App. 1** for histogram of muon momentum).

4. **Z Boson momentum:** How the transverse momentum of the Z boson affects the measurement of the electrons and muons it decays to. If the Z boson had a high transverse momentum, then the conservation of momentum allows the decay products to also have high transverse momenta. Histograms were drawn for the intervals: $p_{Tz} \leq 20\,\text{GeV}$ and $p_{Tz} > 20\,\text{GeV}$ (see **App. 1** for histogram of Z boson momentum).

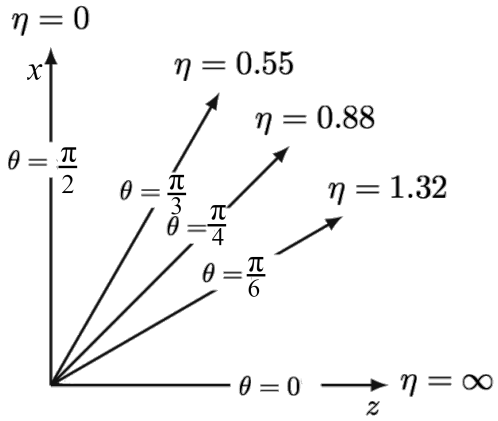

Figure 4: η for some values of θ. Image altered from: (Neutelings, 2017)

3.2 Curve Fitting

For each event that suited the conditions, the invariant mass was calculated from the raw data using equation (1) and histograms were drawn, each with 200 bins (pre-specified intervals that contains values), in the range $0\,\text{GeV} \leq \textit{invariant mass} \leq 200\,\text{GeV}$ (see **App. 1** for the histograms). To the histograms, the Breit-Wigner function, which describes the shape of the peak, and a background function, to account for the photon events, was fitted. The background function consisted of a polynomial of degree 0 and an exponential function. The Breit-Wigner and background function was only fitted in a relevant interval, from $m = 80\,\text{GeV}$ to $m = 100\,\text{GeV}$. The fit has two free parameters, the center and the width.

The center parameter is the center of the peak and was compared to the known

invariant mass of the Z boson by calculating the z-score $z = \frac{x-\mu}{\sigma}$ (Wazir et al., 2012). Within the context of this study, the equation is equal to: $z = \frac{|P_C - Z_m^0|}{\sigma_c}$, where Z_m^0 is the mass of the Z boson, P_C is the centre parameter and σ_c is the uncertainty of the parameter. The z-score is a measurement of how significant the deviation is, that is how well the model (in this case the curve) describes the data and gives an answer in terms of the amount of standard deviations away from the true value. Each σ is associated with a percentage that describes the probability of a random deviation (see **Fig. 5**), so at for example 3σ, there is a 0.1% chance that there is a random deviation, which would suggest that the model is not perfect. The ideal is thus to obtain a small z-score. The z-score was used to analyze the accuracy.

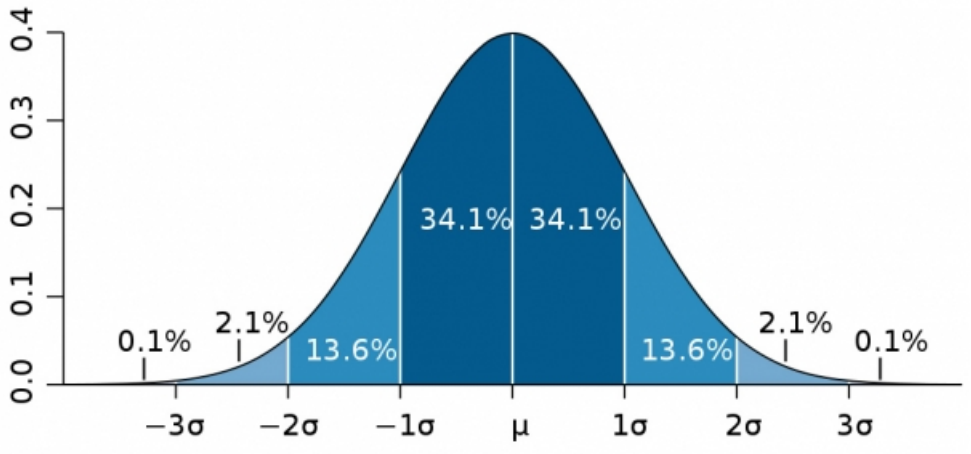

Figure 5: Displays the normal distribution curve and the probability for each σ (Chandler, 2012).

The width parameter which demonstrates the width of the curve will be used to analyze the precision of the detector, as ideally, all events would fall in the bin holding the value 91.2 GeV, thus a narrower fit is more ideal.

4 Results/Analysis

4.1 Muon and Electron Decay Channels

Table 1: Displays the number of entries, center and width parameters for the two histograms, one with muon decay channels and one with electron decay channels (see **App. 1**). The center deviance from Z_m^0 represents the difference (%) between center parameter and invariant mass of the Z boson. Each histogram has 200 bins and the entries refers to the total number of events for the histogram

Decay Channel	Entries	Center	Error	Center deviance from Z_m^0(%)	Z-score	Width	Error
Muon	600071	90.76	(6.03E-03)	-0.47	70.70	5.71	(2.38E-02)
Electron	375216	90.04	(8.90E-03)	-1.26	128.96	6.57	(3.68E-02)

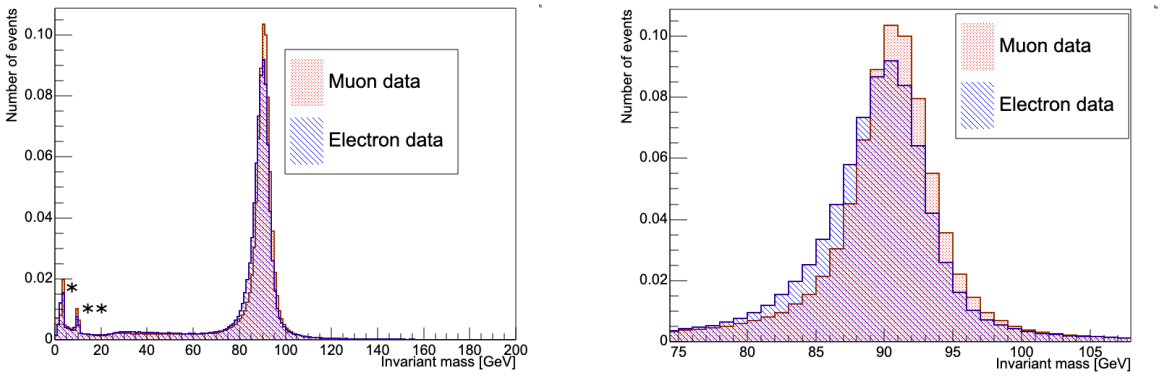

(a) **(b)**

Figure 6: Displays the normalized histograms, when the histograms have been redrawn so the area under the curve equals 1, for the muon(red) and electron(blue) decay channels, where (b) is fixed on the interval $78\,\text{GeV} \leq \textit{invariant mass} \leq 105\,\text{GeV}$.
* represents the invariant mass of the J/ψ meson and ** represents the invariant mass of the upsilon meson.

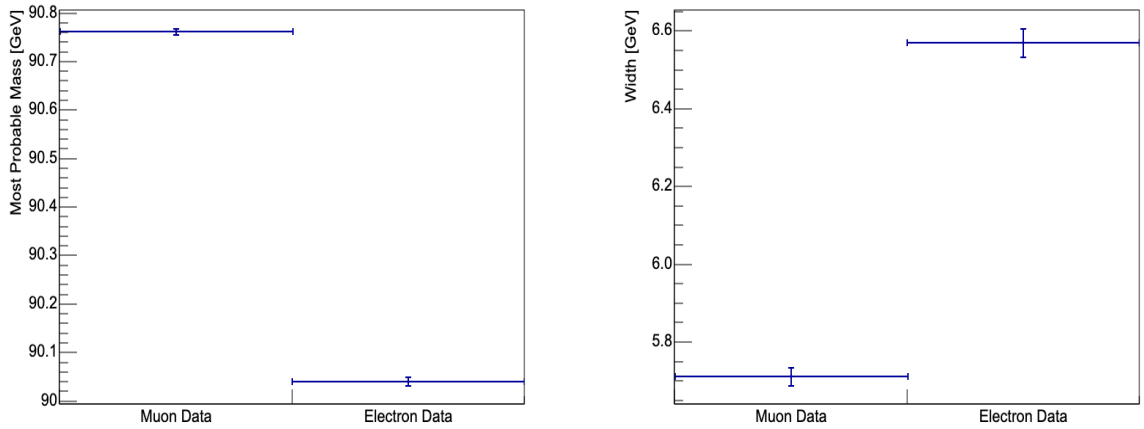

(a) **(b)**

Figure 7: Displays the center (a) and width (b) parameters for the curve fitting of the Breit-Wigner and background function to the histograms for the muon and electron decay channels.

As seen in **Fig. 7a)** and **Tab. 1**, the value of the center parameter for the muon histogram is 0.47% smaller than the invariant mass, compared to the center parameter for the electron histogram which is 1.26% smaller. In **Fig. 7a)** it can also be observed that the error bars do not overlap. Additionally, the center parameter for the muon histogram has a lower z-score compared to the electron histogram. This suggests less accuracy in the measurement of electrons.

The width parameter of the muon histogram is 13.1% less than that of the electron histogram, and the error bars do not overlap, which indicates less precision in the measurement of electron quantities (see **Fig. 7b)**). However, the histogram for the muon events contains 59.9% more entries compared to the histogram for the electron events (see **Tab. 1**). On the other hand, it is noted in **Fig. 6b**) that the muon histogram appears to have proportionally more events in bins covering events with higher invariant mass than the Z boson, as opposed to the electron his-

togram that appears to have more events in bins less than the invariant mass of the Z boson.

4.2 Pseudorapidity

Table 2: The number of entries, center and width parameter of the Breit-Wigner and background function for the five histograms (see **App. 1**) containing events for five different intervals of $|\eta|$ for the moun decay channel.

Pseudorapidity (η)	Entries	Center	Error	Center deviance from Z_m^0(%)	Z-score	Width	Error
$\|\eta\| \leq 0.25$	8652	90.73	(3.90E-02)	-0.51	11.87	4.60	(1.28E-01)
$0.25 < \|\eta\| \leq 0.5$	3445	90.88	(7.63E-02)	-0.34	4.06	4.81	(2.47E-01)
$0.5 < \|\eta\| \leq 1$	22278	90.78	(3.00E-02)	-0.45	13.65	5.42	(1.04E-01)
$1 < \|\eta\| \leq 1.5$	12954	90.67	(5.20E-02)	-0.57	10.03	6.58	(2.29E-01)
$1.5 < \|\eta\|$	41059	90.72	(3.01E-02)	-0.51	15.44	6.86	(1.26E-01)

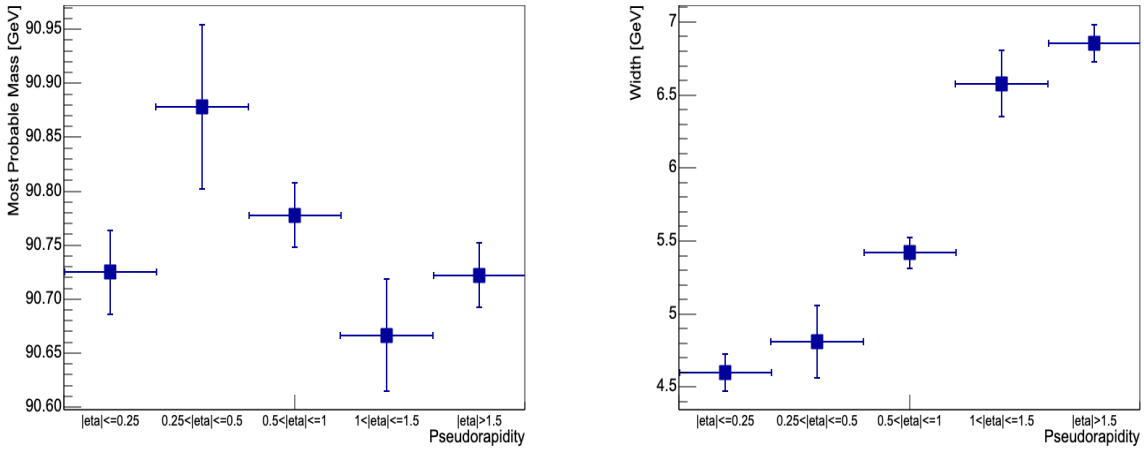

(a) **(b)**

Figure 8: The centre (a) and width (b) parameters for the Breit Wigner and backround function for the 5 histograms displaying the mass of the Z boson when $|\eta| \leq 0.25$, $0.25 < |\eta| \leq 0.5$, $0.5 < |\eta| \leq 1$, $1 < |\eta| \leq 1.5$ and $|\eta| > 1.5$.

In **Fig. 8a)** and **Tab. 2**, it can be observed that the smallest z-score and center deviance from mass occurs for $0.25 < |\eta| \leq 0.5$, but its error bars overlap with the bin for $0.5 < |\eta| \leq 1$ which has a z-score of 13.65. For $|\eta| \leq 0.25$, the error bars overlap with all other points except $0.25 < |\eta| \leq 0.5$ (see **Fig. 8a)**). Furthermore, it can also be seen in **Fig. 8a)** that the three bins $0.5 < |\eta| \leq 1$, $1 < |\eta| \leq 1.5$ and $|\eta| > 1.5$ have overlapping error bars with at least 2 other bins. No trend can therefore be observed regarding the effect of pseudorapidity on the accuracy of the ATLAS Detector.

It can be observed that the width parameter increases as the absolute value of the pseudorapidity increases. For example, there was a 21.4% increase from $0.5 < |\eta| \leq 1$ to $1 < |\eta| \leq 1.5$. The error bars for $|\eta| \leq 0.25$ and $0.25 < |\eta| \leq 0.5$ overlap, and the same is observed for $1 < |\eta| \leq 1.5$ and $|\eta| > 1.5$. The width parameter for $0.5 < |\eta| \leq 1$ does not have overlapping error bar with any other point. The increase in width suggests a decrease in precision.

4.3 Muon Momentum

Table 3: The number of entries, the center and width parameter of the Breit-Wigner and background function for the five histograms (see **App. 1**) with five different transverse momentum, P_T, (GeV) selections of the muons.

P_T (GeV)	Entries	Center	Error	Center deviance from Z_m^0(%)	Z-score	Width	Error
$P_T \leq 30$	71163	90.48	(2.31E-02)	-0.77	30.47	5.33	(7.78E-02)
$30 < P_T \leq 40$	61880	90.47	(1.68E-02)	-0.79	42.87	5.50	(6.70E-02)
$40 < P_T \leq 45$	35749	89.83	(1.48E-02)	-1.49	91.74	5.95	(6.15E-02)
$45 < P_T \leq 50$	14198	93.71	(2.34E-02)	+2.76	107.53	4.39	(6.27E-02)
$50 < P_T$	11247	91.42	(5.68E-02)	+0.25	4.05	6.11	(2.22E-01)

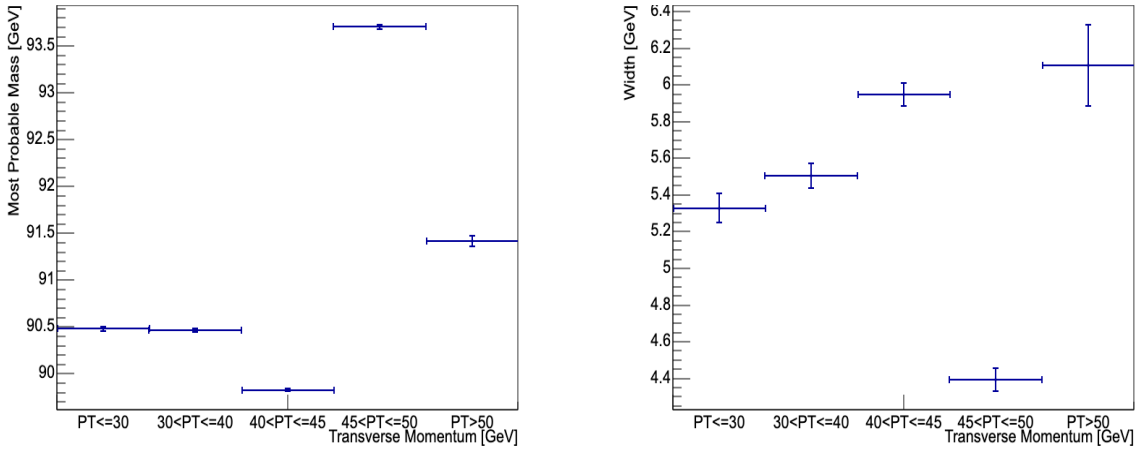

(a) **(b)**

Figure 9: The center (a) and width (b) parameters of the peak showing the mass of the Z boson for the five histograms with five different intervals of muon momentum.

As visualized in **Fig. 9a)**, the error bars do not overlap except for the two bins $p_T \leq 30\,\text{GeV}$ and $30\,\text{GeV} < p_T \leq 40\,\text{GeV}$. For the first four bins, it can be observed that the z-score increases as the muon momentum increases. For example, from $30\,\text{GeV} < p_T \leq 40\,\text{GeV}$ to $40\,\text{GeV} < p_T \leq 45\,\text{GeV}$ there was 114% increase. This suggests a decrease in accuracy as the momentum of the muon's increases. However, for $p_T > 50\,\text{GeV}$ it is noted that the z-score is 4.05, which is 96% smaller than for $40\,\text{GeV} < p_T \leq 45\,\text{GeV}$ (see **Tab.3**).

The width parameter increases for the first 3 bins, however, the two bins for when $p_T \leq 30\,\text{GeV}$ and $30\,\text{GeV} < p_T \leq 40\,\text{GeV}$ have overlapping error bars (see **Fig. 9b)**). For $45\,\text{GeV} < p_T \leq 50\,\text{GeV}$, the peak was the narrowest, being 26.1% narrower than for when $40\,\text{GeV} < p_T \leq 45\,\text{GeV}$. For $p_T > 50\,\text{GeV}$ the peak is the widest, being 2.7% wider than $40\,\text{GeV} < p_T \leq 45\,\text{GeV}$ (see **Fig. 9a)**), and the error bars only overlap with the bin holding the values for $40\,\text{GeV} < p_T \leq 45\,\text{GeV}$ which indicates a decreasing precision for increasing muon momenta.

4.4 Z Boson Momentum

Muon Decay Channel

Table 4: The number of entries for the two histograms (see **App. 1**) with two different intervals of Z boson momentum, P_{Tz}, (GeV) and the center- and width parameter after fitting the Breit-Wigner and background function. Only for the muon decay channel.

P_{Tz} (GeV)	Entries	Center	Error	Center deviance from Z_m^0(%)	Z-score	Width	Error
$P_{Tz} \leq 20$	350181	90.74	(7.20E-03)	-0.49	62.05	5.63	(2.86E-02)
$20 < P_{Tz}$	249890	90.81	(9.93E-03)	-0.42	38.22	5.88	(3.89E-02)

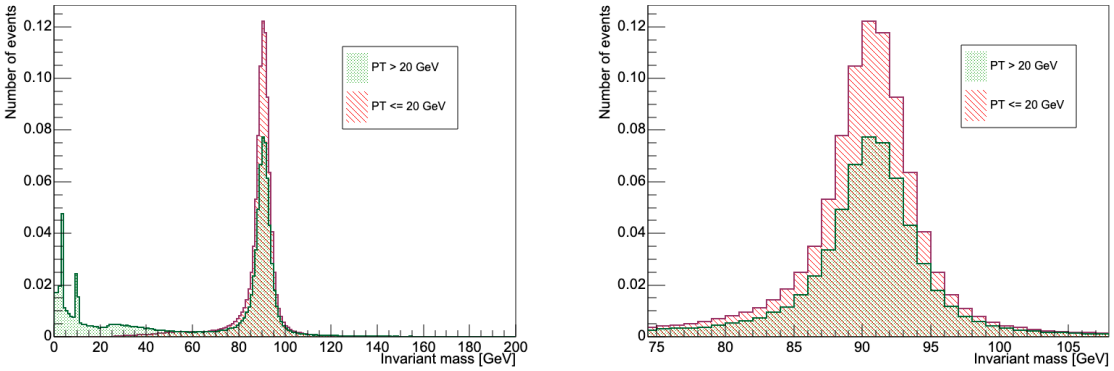

(a) **(b)**

Figure 10: The two normalized histograms for when $P_{Tz} \leq 20\,\text{GeV}$ (red) and $P_{Tz} > 20\,\text{GeV}$ (green) for the muon decay cannels.

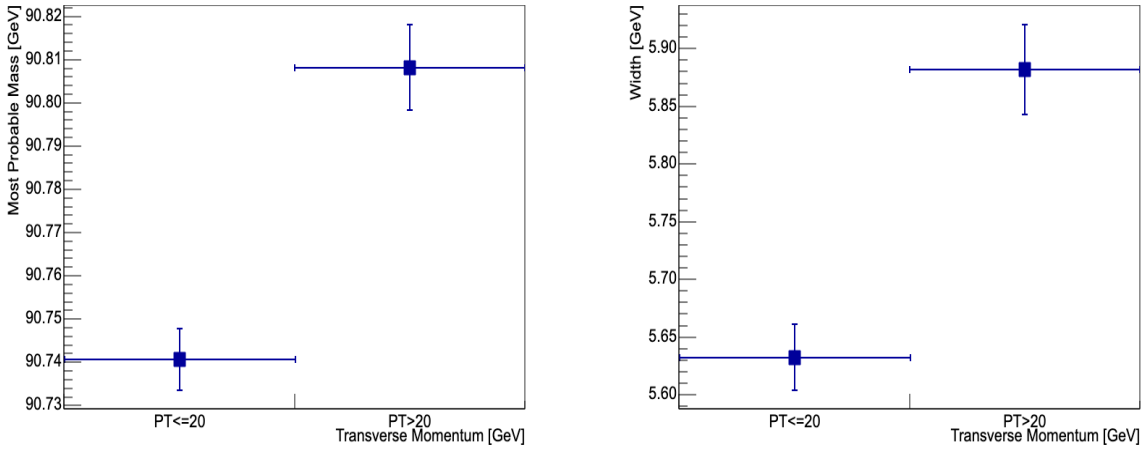

(a) **(b)**

Figure 11: The center and width parameter of the Breit-Wigner and background function fitted to the two histograms with muon decay channels for different momenta of the Z boson created in the collision.

In **Tab. 4** and **Fig. 11a)**, it can be seen that the z-score for when $p_{Tz} > 20\,\text{GeV}$ is 38.4% smaller than the z-score of $p_{Tz} \leq 20\,\text{GeV}$. Furthermore, the error bars for the center parameter do not overlap (see **Fig. 11a)**). This suggests an increase

in accuracy as the Z boson momentum increases. The width parameter of the Breit-Wigner function for the histogram containing events where the Z boson had a momentum $p_{Tz} \leq 20\,\text{GeV}$ was 4.4% smaller compared to when the Z boson had a momentum $p_{Tz} > 20\,\text{GeV}$, and the error bars do not overlap (see **Fig. 11b)**). This implies less precise measurements when the Z boson has a high transverse momentum. Furthermore, when $p_{Tz} > 20\,\text{GeV}$, there were more events with the J/ψ meson and upsilon meson compared to when $p_{Tz} \leq 20\,\text{GeV}$ (see **Fig. 10a)**).

Electron Decay Channel

Table 5: Displays the number of entries for the two histograms (see **App. 1**) with two intervals of Z boson momenta, P_{Tz}, (GeV) containing only electron decay channels. The center and width parameter were generated after fitting the Breit-Wigner and background function.

Z Boson Momentum (P_{Tz})	Entries	Center	Error	Center deviance from Z_m^0(%)	Z-score	Width	Error
$P_{Tz} \leq 20$	214348	90.00	(1.25E-02)	-1.30	95.18	6.57	(4.72E-02)
$20 < P_{Tz}$	160868	90.12	(1.54E-02)	-1.17	69.16	6.56	(5.83E-02)

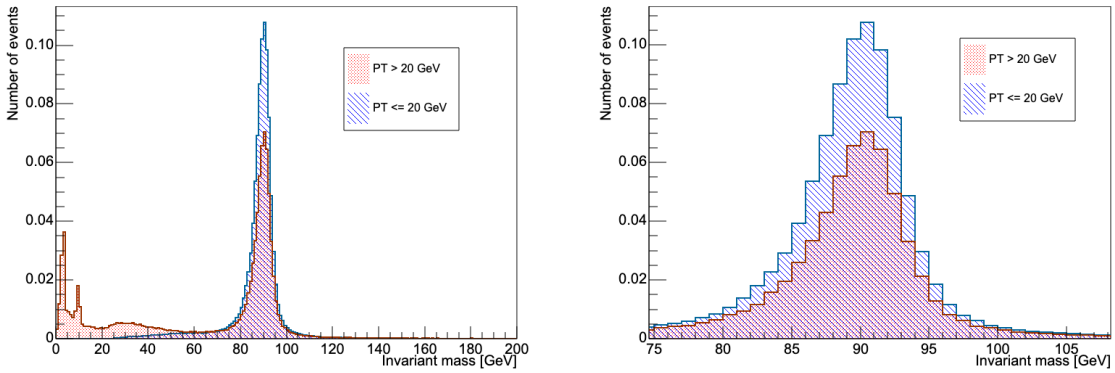

(a) **(b)**

Figure 12: Normalized histograms containing electron decay channels covering the intervals $P_{Tz} \leq 20\,\text{GeV}$ (blue) and $P_{Tz} > SI20$ (red).

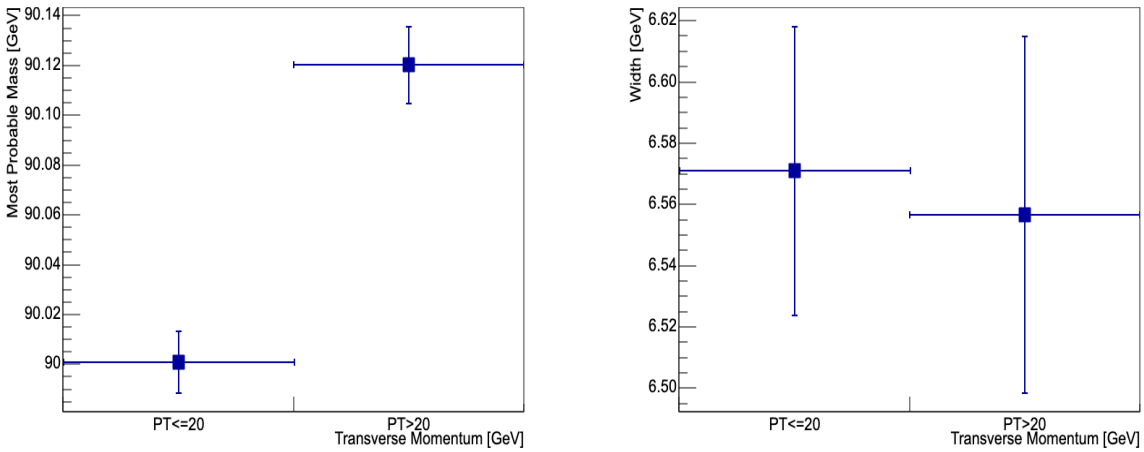

(a) **(b)**

Figure 13: Displays the center (a) and width (b) parameter for the two histograms with different values of Z boson momenta. Only the electron decay channel is included.

As can be observed in **Fig. 13a)** and **Tab. 5** the center parameter for when $p_{Tz} \leq 20\,\text{GeV}$ is 1.30% smaller than the invariant mass of the Z boson compared to when $p_{Tz} > 20\,\text{GeV}$, where the center parameter deviance is 1.17% smaller. The error bars for the center parameter do not overlap (see **Fig. 13b)**). Additionally, the z-score of $p_{Tz} \leq 20\,\text{GeV}$ is 37.6% greater than that of $p_{Tz} > 20\,\text{GeV}$ (see **Tab. 5**). This suggests an increase in accuracy as the momentum of the Z boson increases. Furthermore, it can be seen in **Fig. 13b)** that the width parameters have overlapping error bars, thus no trend can be observed regarding the precision. Lastly, the histogram for $p_{Tz} \leq 20\,\text{GeV}$ contains fewer events where the J/ψ meson and upsilon meson were created than the histogram for $p_{Tz} > 20\,\text{GeV}$ (see **Fig. 12a)**).

5 Conclusion

The conclusion drawn is that the ATLAS Detector is more accurate and precise when measuring muon quantities compared to electron quantities. For increasing pseudorapidities for the muon decay channel, the accuracy of the ATLAS Detector is not affected whereas the precision decreases. As the muon momentum increased, the accuracy and precision of the detector decreased. For both muon and electron decay channels, the accuracy increased as the momentum of the Z boson increased. It can also be conlcuded that for the muon decay channel, a high Z boson momentum affects the precision negatively, whereas there was no effect for the electron decay channel.

6 Evaluation of Methods

As seen in **Tab. 1-5**, the histograms compared contain different amount of entries. For example, the histogram for when $|\eta| > 1.5$ contains 375% more entries than the histogram for $|\eta| \leq 0.25$. The amount of events in a histogram affects the error for each bin, which therefore affects the curve fitting and thus the parameter and errors for each parameter.

Furthermore, two functions were fitted to the histogram, the Breit-Wigner, which describes the shape of the peak around the invariant mass of the Z boson, and a background function consisting of an exponential and 0 degree polynomial to account for all the photon events. However, the peak obtained is wider around the edges, and this is due to that the ATLAS Detector makes errors when measuring, and this error is Gaussian (Ohm & Ripellino, 2019). In order to fit the true shape of the peak, a Gaussian component should have been included in the function.

For the effect of muon momentum and pseudorapidity on the accuracy and precision, five different intervals were investigated for each. However, only two intervals were investigated for the effect Z boson momentum has on the precision. This means that for each event, there were only two histograms available, whereas if a more detailed selection was done with histograms for various intervals, it would be possible to better classify the events and thus study the topic more in detail.

The mass of the Z boson is known to high precision due to that it has been calculated many times from raw data. For this paper, not enough data was used to reach the same precision as the known invariant mass.

Furthermore, despite that 14.9×10^6 collisions were looped through, there are not many collisions where the Z boson has been created, which can be seen in **Tab. 1** were the total amount of electron and muon entries add up to 975287 events. There might not be enough events for a scenario to be able to see a difference, or there might not be enough data to reflect the true difference. Thus, if more data is released in the future, it could be included for a more representative investigation.

7 Discussion

For this paper, one scenario investigated was how the momentum of the Z boson affects the accuracy and precision. The explination provided was that by conservation of momentum, if the Z boson has a high momentum then the particles may also have a high momentum. However, it is important to know that it is the sum of the two momenta of the decay products that is equal to, thus a high Z boson momentum does not garuantee that both particles had high momenta. Additionally, for the electron decay channels, the electromagnetic calorimeter accounts for one measurement, thus this could explain why there was no difference in precision.

As the ATLAS detector measures the quantities of muons in the inner detector and the muon spectrometer by bending their path using a magnetic field, it was expected that for increasing muon momenta the accuracy and precision would decrease since it becomes more difficult to bend the path of the muons thus affecting the measurements. As mentioned, there appeared to be a general trend with the exception of some values, such as $45\,\text{GeV} < p_T \leq 50\,\text{GeV}$ in **Fig. 9b)**. This could be due to the absence of the Gaussian component of the curve fitted to the histograms.

The difference in accuracy and precision for muon and electron decay channels could be due to the electromagnetic calorimeter and energy measurement. Lastly, it was expected that the pseudorapidity would affect the precision because the ATLAS Detector makes use of a magnet system with different strengths (ATLAS experiment, 2019) thus a variation in the magnetic field was expected, however it was not sure how the precision would be affected and where the variations occurred. It was also expected that pseudorapidity would have an effect on the accuracy of the ATLAS Detector, but this was not the case.

It was observed for both of the muon and electron decay channels that when $p_{Tz} > 20\,\text{GeV}$, there were more events where the J/ψ meson and upsilon meson were created compared to when $p_{Tz} \leq 20\,\text{GeV}$. This could be due to the selection of events by the ATLAS Detector. As the J/ψ meson and upsilon meson have low invariant masses, if the mesons have high energies, it means that the electrons and muons also will have higher energies, thus the collision will appear as interesting.

For future investigations, one could include more and narrower intervals for the effect of Z boson momenta on the precision. It could also be studied how the preci-

sion and accuracy varies for various intervals of ϕ, the azimuthal angle. Additionally, the potential variation of precision and accuracy in the electromagnetic calorimeter could also be examined.

Due to that the ATLAS Detector is used in for example the search of dark matter and new particles, it is important to know how the precision varies depending on the magnetic field. The knowledge of variations in the accuracy and precision is important to operating particle physicists at CERN, and may help humankind to better understand the universe in the future.

8 Acknowledgments

I would like to thank Christian Ohm and Giulia Ripellino from KTH, Alba Nova, for their support, guidance and for explaining all of the concepts while still encouraging me to think independently. I would also like to thank my school supervisors Felicia Dinnétz and Per-Olof Freerks, for their input.

9 References

ATLAS experiment. (2019). Calorimeter. Retrieved 2019-03-14 from:
https://atlas.cern/discover/detector/calorimeter
ATLAS experiment. (2019). Detector and technology. Retrieved 2019-03-14 from:
https://atlas.cern/discover/detector
ATLAS experiment. (2019). Magnet system. Retrieved 2019-03-31 from:
https://atlas.cern/discover/detector/magnet-system
ATLAS experiment. (2019). Mass/Invariant mass. Retrieved 2019-03-31 from:
https://atlas.cern/glossary/mass-invariant-mass
ATLAS experiment. (2019). Muon spectrometer. Retrieved 2019-03-14 from:
https://atlas.cern/discover/detector/calorimeter
ATLAS experiment. (2019). The inner detector. Retrieved 2019-03-14 from:
https://atlas.cern/discover/detector/inner-detector
Cern. (2019). ATLAS. Retrieved 2019-03-14 from:
https://home.cern/science/experiments/atlas
Chandler, D., L. (2012). [Untitled image of normal distribution]. Retrieved:
2019-03-29 from http://news.mit.edu/2012/explained-sigma-0209
Delmastro, M. (2012). [Untitled Image of particles detected in the ATLAS detector]. Retrieved 2019-03-29 from:
https://www.borborigmi.org/2012/07/20/rivelatori-di-particelle-a-lhc-la-serie-completa/
Hallsjö, S., P. (2014). The atlas detector and the definition of the orthogonal Cartesian coordinate system. [Image]. Retrieved 2019-03-30 from:
https://www.researchgate.net/figure/The-atlas-detector-and-the-definition-of-the-\
orthogonal-Carte-sian-coordinate-system_fig4_283697708
Hamper, C. (2014). Higher Level Physics. Essex: Pearson Education, Inc.
International masterclasses. (N/A). More About the Z boson. Retrieved 2019-03-15 from:
https://atlas.physicsmasterclasses.org/exercises/ATLAS-2015/en/zpath_lhcphysics2.
htm
Neutelings, I. (2017). [Untitled image of pseudorapidity]. Retrieved 2019-03-25 from:
https://wiki.physik.uzh.ch/cms/latex:exampe_eta
Tanabashi, M. et al. (2019). Particle Data Group. Phys. Rev. D 98, 030001.
M. Tanabashi et al. (Particle Data Group), Phys. Rev. D 98, 030001 (2018) Tripathee, A. (2017). [Untitled image of Feynman diagram]. Retrieved 2019-03-31 from:
https://www.physicsden.org/problem/using-cms-open-data-to-measure-z-boson-mass
The ATLAS Colaboration et al., (2008). The ATLAS Experiment at the CERN Large Hadron

Collider. IOP Science, 3(08). 14. doi: 10.1088/1748-0221/3/08/s08003
Wazir, I. Garry, T. (2012). Higher Level Mathematics. Essex: Pearson Education, Inc.

Personal comment: Giulia Ripellino (2019). KTH, Alba Nova/Particle Physics dept. Roslagstullsbacken 21 s-114 21, Stockholm Sweden. Ph.: +46 73 765 24 72. giuliar@kth.se
Personal comment: Christian Ohm. (2019). KTH, Alba Nova/Particle Physics dept. Roslagstullsbacken 21 s-114 21, Stockholm Sweden. Ph.: +46 73 644 14 11. chohm@kth.se

Appendix 1

Muon and Electron Histograms

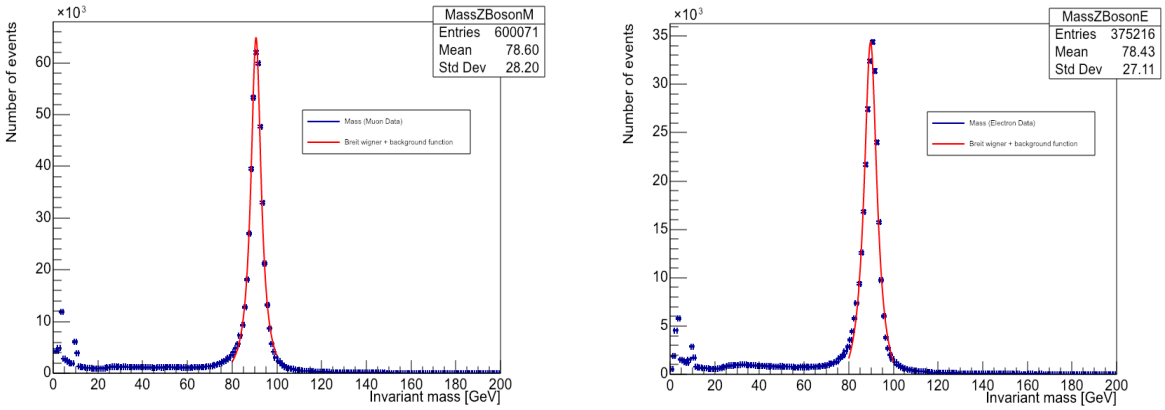

(a) **(b)**

Figure 14: Displays the number of events for each invariant mass for the muon decay channels only (a), electron decay channels only (b) with the Breit-Wigner and background function fitted. Each histogram has 200 bins.

Pseudorapidity Histograms

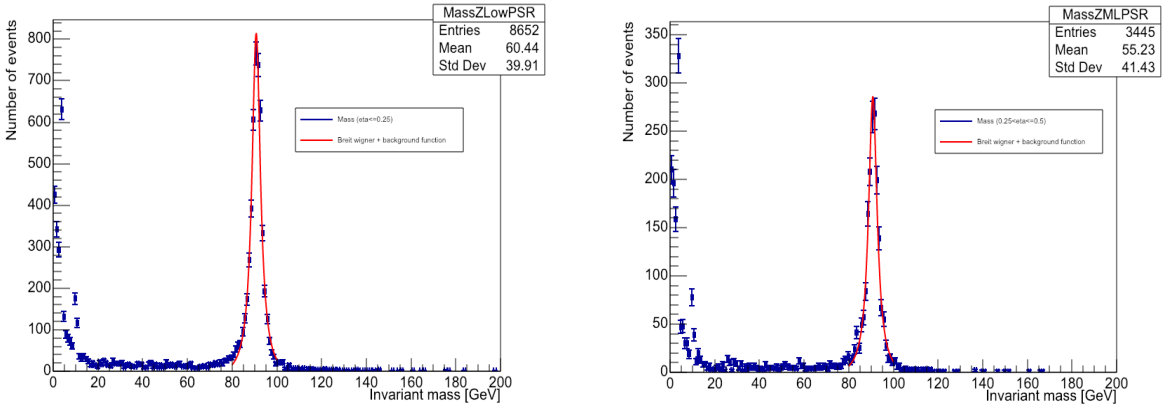

(a) **(b)**

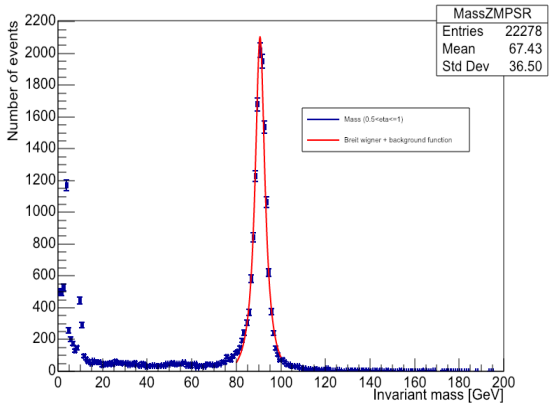

(c)

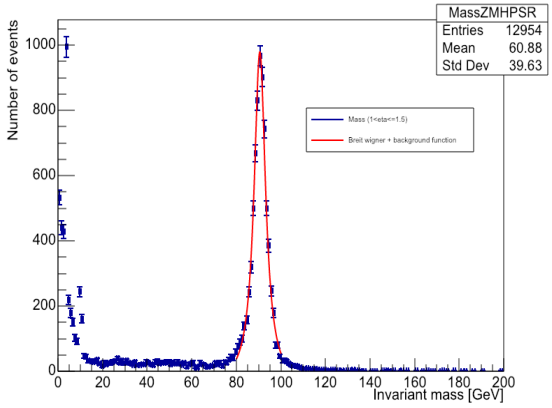

(d)

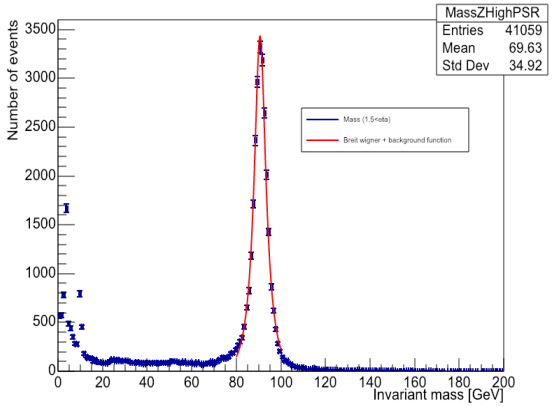

(e)

Figure 15: The different histograms for 5 intervals of $|\eta|$: $|\eta| \leq 0.25$ (a), $0.25 < |\eta| \leq 0.5$ (b), $0.5 < |\eta| \leq 1$ (c), $1 < |\eta \leq 1.5$ (d) and $|\eta| > 1.5$ (e). The Breit-Wigner and background function has been fitted to all 5 histograms and each has 200 bins.

Muon Momentum Histograms

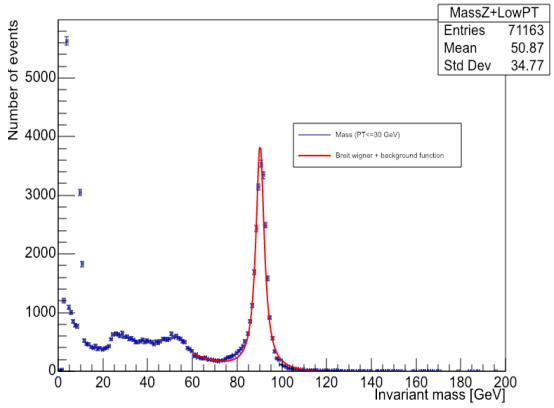

(a)

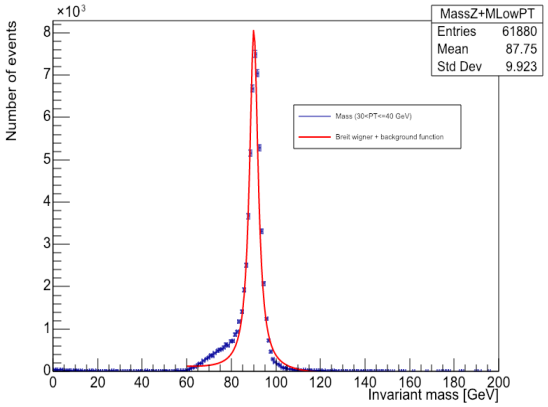

(b)

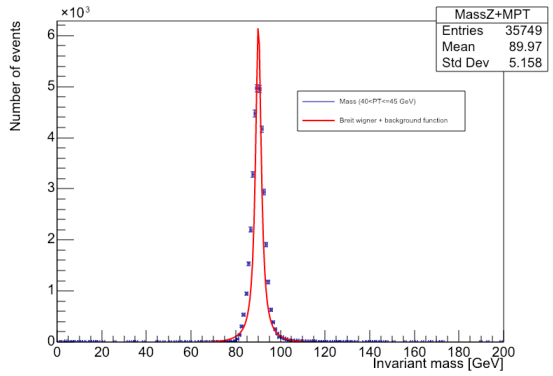

(c)

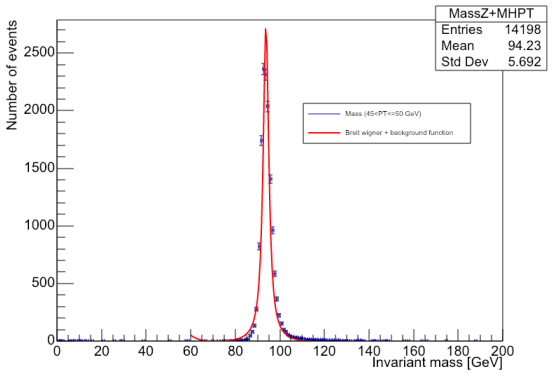

(d)

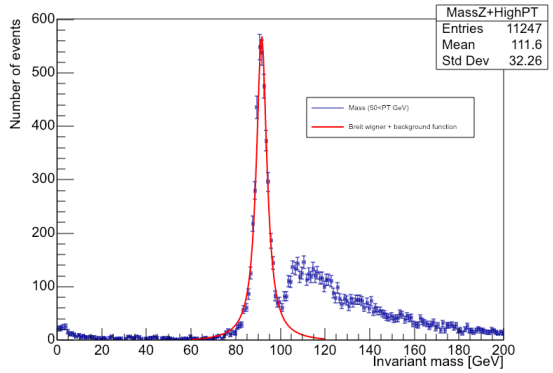

(e)

Figure 16: Displays the number of events for each invariant mass (GeV) for the muon transverse momentum intervals $P_T \leq 30\,\text{GeV}$ (a), $30\,\text{GeV} < P_T \leq 40\,\text{GeV}$ (b) $40\,\text{GeV} < P_T \leq 45\,\text{GeV}$ (c), $45\,\text{GeV}45 < P_T \leq 50\,\text{GeV}$ (d) and $P_T > 50\,\text{GeV}$(e). There are 200 bins for each histogram and the Breit-Wigner and background function has been fitted in the interval 80-100 GeV.

Z Boson Momentum Histograms

Muon Decay Channel

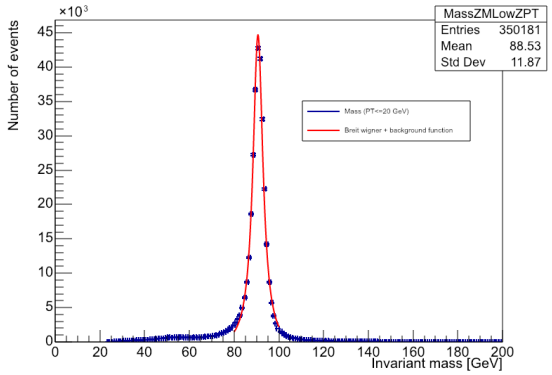

(a)

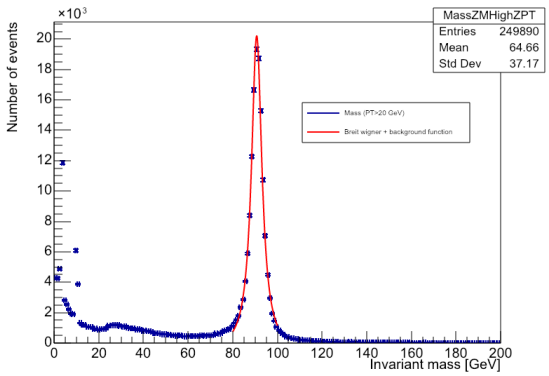

(b)

Figure 17: The number of events against each invariant mass (GeV), a total of 200 bins for each histogram, for the muon decay channels with Z boson momentum intervals $P_{Tz} \leq 30\,\text{GeV}$ (a) and $P_{Tz} > 30\,\text{GeV}$. Fitted with the Breit-Wigner and background function

Electron Decay Channel

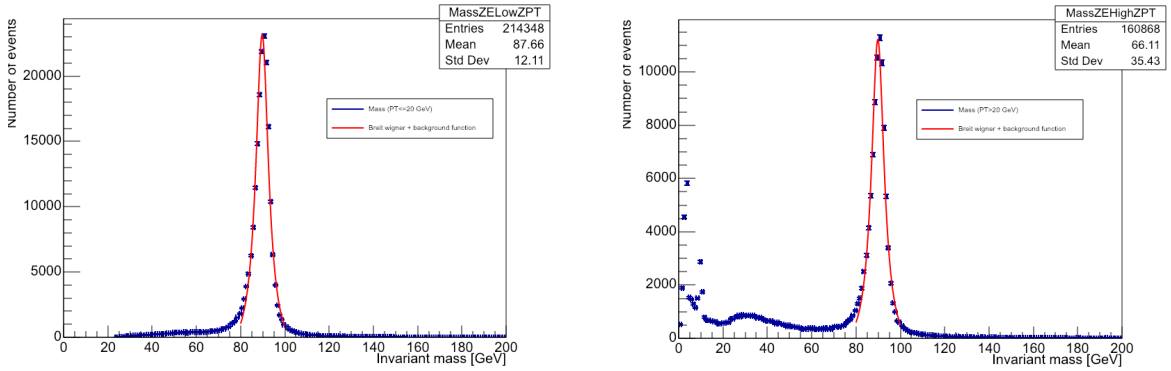

(a) **(b)**

Figure 18: The number of events against the invariant mass (GeV) for two different Z boson momentum intervals, $P_{Tz} \leq 30\,\text{GeV}$ (a) and $P_{Tz} > 30\,\text{GeV}$ (b), containing electron events only and 200 bins each. The Breit-Wigner and background function is fitted.

Momentum of Muons and Z bosons

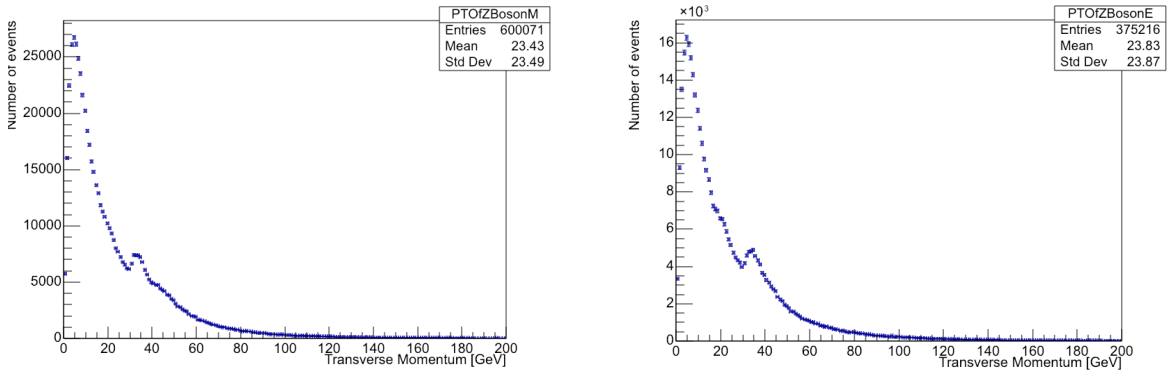

(a) **(b)**

Figure 19: Displays the number of events against the momentum (GeV) of the Z boson for the muon decay channel (a) and the electron decay channel (b).

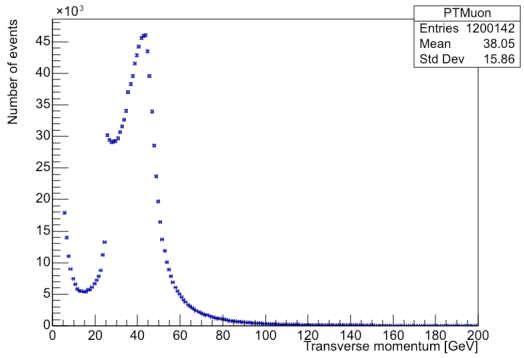

Figure 20: Displays the number of events against the momentum (GeV) of the muons

Appendix 2

As mentioned in the methodology, a programme was written using Python 3 and ROOT in order to loop through all events in the most efficient way. The code can be found at `https://github.com/mariamelise/OpenDataZmassLab/blob/master/the-exercise/3-TheTask-ZbosonMass.ipynb`